 Related Commentary, page 2265

Adrenal glucocorticoids have a key role in circadian resynchronization in a mouse model of jet lag

Silke Kiessling, Gregor Eichele, and Henrik Oster

Department Genes and Behavior, Max Planck Institute for Biophysical Chemistry, Göttingen, Germany.

Jet lag encompasses a range of psycho- and physiopathological symptoms that arise from temporal misalignment of the endogenous circadian clock with external time. Repeated jet lag exposure, encountered by business travelers and airline personnel as well as shift workers, has been correlated with immune deficiency, mood disorders, elevated cancer risk, and anatomical anomalies of the forebrain. Here, we have characterized the molecular response of the mouse circadian system in an established experimental paradigm for jet lag whereby mice entrained to a 12-hour light/12-hour dark cycle undergo light phase advancement by 6 hours. Unexpectedly, strong heterogeneity of entrainment kinetics was found not only between different organs, but also within the molecular clockwork of each tissue. Manipulation of the adrenal circadian clock, in particular phase-shifting of adrenal glucocorticoid rhythms, regulated the speed of behavioral reentrainment. Blocking adrenal corticosterone either prolonged or shortened jet lag, depending on the time of administration. This key role of adrenal glucocorticoid phasing for resetting of the circadian system provides what we believe to be a novel mechanism-based approach for possible therapies for jet lag and jet lag–associated diseases.

Introduction

The term *jet lag* describes a set of physiological and psychological perturbations experienced when internal circadian rhythms and external time are out of synchrony, for example, after traveling in a jet plane across multiple time zones (1, 2). It is characterized by decreased alertness, nighttime insomnia, poor overall performance (3), impaired cognitive skills (4), loss of appetite, depressed mood, reduced psychomotor coordination, and gastrointestinal disturbances (5). The severity and extent of these symptoms depend on the direction and speed of travel and the number of time zones crossed (5–8). Individuals exposed to chronic jet lag may experience accelerated malignant growth (9) and temporal lobe atrophy combined with spatial cognitive deficits (10). Rodents subjected to chronic jet lag suffer from cardiomyopathies (11) and hastened death upon aging (12).

Circadian clocks are oscillators driven by interlocked positive and negative transcriptional/translational feedback loops. The clock transcriptional activators circadian locomotor output cycles kaput (CLOCK) and aryl hydrocarbon receptor nuclear translocator–like; (ARNTL; also referred to as BMAL1) turn on period (*Per1*, *Per2*, and *Per3*) and cryptochrome (*Cry1* and *Cry2*) genes. PER and CRY proteins are negative regulators repressing CLOCK/ARNTL-mediated transactivation (13–15). A second loop involves positive and negative regulation of *Arntl* expression through RAR-related orphan receptor α (RORα) and nuclear receptor subfamily 1, group D, member 1 (NR1D1; also known as REV-ERBα), respectively (16). The transcription factor D site albumin promoter binding protein (DBP) regulates rhythmic activation of downstream target genes (17), thereby serving as relay mediating the output of the circadian oscillator.

The master pacemaker of the hypothalamic suprachiasmatic nuclei (SCN) and also peripheral oscillators all rhythmically express clock genes (18). The SCN appears to synchronize peripheral oscillators present in, for example, the cerebral cortex (19, 20), the retina (21), the liver (22), the kidney (23), and the pancreas (24–27) through hormonal and neuronal pathways (27, 28). Peripheral clocks translate clock time into physiologically meaningful signals via rhythmic activation of clock-controlled genes (29, 30). The temporal disorganization of the circadian system during jet lag is likely to disrupt overall physiological coordination and, hence, be the cause of most jet lag–associated symptoms (6). Yamazaki et al. have found that during jet lag, *Per1* expression rhythms reentrain faster in the SCN than in any of the other tissues examined (22). Similar findings were reported by Davidson et al. for *Per2* (31). Reddy et al. found a dissociation of period and cryptochrome gene expression rhythms during jet lag and postulated that the slower-adapting cryptochrome rhythm acts as a rate-limiting factor for behavioral adaptation (32). Collectively, the results of these studies, which included a limited number of tissues and circadian genes, suggest that coordination of clock gene expression is globally disrupted during jet lag. This prompted us to systematically examine reentrainment of the major components of positive and negative branches of the circadian feedback loop in a variety of tissues. We found that the rate of clock gene reentrainment varied among both genes and tissues.

It remains unclear which factors mediate the organismal process of reentrainment. Adrenal glucocorticoids (GCs) can reset peripheral clocks (33), and the adrenal circadian clock regulates the rhythmic release of GCs into the blood (34). Sage and colleagues showed that rhythmicity of GCs influences photic entrainment of locomotor activity in rats (35). This led us to hypothesize that the adrenal clock coordinates circadian reentrainment during jet lag by gradually adjusting GC rhythms. We discovered that genetic ablation of the adrenal clock accelerated the rate of reentrainment. Timed application of metyrapone (MET), an inhibitor of adrenal GC synthesis, evoked a shift in the GC rhythmicity and — depending on

Conflict of interest: The authors have declared that no conflict of interest exists.
Citation for this article: *J Clin Invest.* 2010;120(7):2600–2609. doi:10.1172/JCI41192.

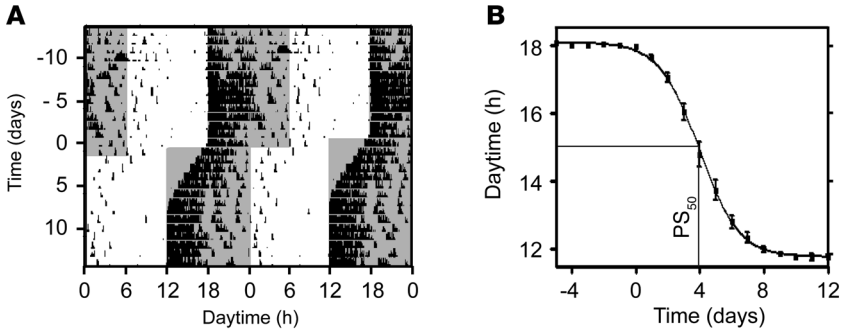

Figure 1
Behavioral entrainment during jet lag. (**A**) Representative double-plotted actogram of a mouse before and after 6-hour LD phase advance applied at day 1. Tick marks represent wheel running activity; gray shading denotes dark lighting conditions. (**B**) Average onset of mice ($n = 9$) during jet lag. PS_{50} (4.0 ± 0.1 days) was defined as the time at which half the phase shift was completed. All values are average ± SEM.

the time point of drug application — resulted in either acceleration or deceleration of behavioral adaptation to the new time zone. We conclude that the adrenal circadian clock, through control of GC rhythms, is a major regulator of reentrainment to jet lag.

Results

Differential response of circadian clock gene expression in the SCN during jet lag. Mice were entrained to a light-dark (LD) cycle of 12 hours light, 12 hours dark. Their running-wheel activity was restricted to the dark phase (Zeitgeber time 12 to 24; ZT12–ZT24), as expected for nocturnal animals. Advancing the LD cycle by 6 hours (which simulates eastward traveling) evoked a gradual adaptation of running-wheel activity to the changed light regimen. This transition was completed after 8–9 days (Figure 1A). We determined locomotor activity onsets before and after the shift. Onset resetting followed a sigmoid curve, and a 50% phase shift (PS_{50}) was reached at 4.0 ± 0.1 days (Figure 1B).

Because locomotor activity is believed to be driven by the circadian pacemaker of the SCN (36–39), adaptation to a new time zone should be reflected by changes of clock gene expression in the SCN. Hence, we used in situ hybridization (ISH) to determine jet lag–evoked changes in the transcription profiles of 5 canonical clock genes: *Per1*, *Per2*, *Dbp*, *Nr1d1*, and *Arntl*. Results of densitometric quantifications of autoradiographs of coronal sections through the SCN are depicted in Figure 2A. Before the shift (day 0), transcripts of *Per1*, *Per2*, and *Dbp* showed rhythmic expression with peak levels around the middle of the day (ZT4–ZT10; Figure 2A, top row). *Arntl* transcript levels were highest around ZT16, while *Nr1d1* mRNA levels peaked around the ZT0 night/day transition. At 12 days after the shift, the transcript rhythms had fully adapted to the new LD cycle (Figure 2A). Circadian transcript profiles of the different clock genes at intermediary time points showed marked differences in their individual adaptation characteristics. To quantify the kinetics of adaptation of clock gene expression, we determined mRNA peaks by sine wave regression (Figure 2A). The rhythmicity of circadian expression was verified using CircWave software (ref. 34 and Supplemental Table 1; supplemental material available online with this article; doi:10.1172/JCI41192DS1). The time point of peak expression for each gene and day was determined. To facilitate a direct comparison of resetting of expression rhythms of different clock genes, peak times at days 2, 3, 4, and 12 were plotted relative to those at day 0 (Figure 2B). Similar to our activity onset results (Figure 1B), resetting of clock gene expression peaks followed sigmoid kinetics, with full reentrainment reached between day 3 (*Per2*) and day 8 (*Nr1d1*). PS_{50} values revealed a marked difference in adaptation kinetics among the different clock genes (Figure 2C). Consistent with previous work (22), period genes rapidly adapted to the new light schedule. Importantly, other clock genes showed a considerably slower rate of adaptation, more closely reflecting that seen for running-wheel activity (Figure 2C).

Peripheral clocks vary in their rate of adjustment during jet lag. In order to determine the rate of adaptation of peripheral clocks in mice subjected to jet lag conditions, we measured clock gene expression by quantitative real-time PCR (qPCR; adrenal, kidney, liver, and pancreas) or by ISH (somatosensory cortex) at days 0, 2, 3, 4, and 8 or 12 following a 6-hour advance of the LD cycle. Sine wave regression and *F* testing using CircWave software (34) showed that gene expression patterns were rhythmic at all times (Supplemental Figure 1 and Supplemental Table 1). PS_{50} values were determined as described above for the SCN; values for all tissues examined are shown in Figure 3. Somatosensory cortex and SCN showed a similar pattern of clock gene adaptation (compare Figure 2C and Figure 3A). In both cases, we observed a rapid response of *Per1* and *Per2*, followed by a slower response for *Dbp*, *Arntl*, and *Nr1d1*. The rate of adjustment of period genes was not as rapid in non-neuronal tissues, except for the adrenal. *Per2* shifted fastest in kidney and liver, whereas *Arntl* shifted slowest and *Per1* shifted slower, comparable to *Dbp* and *Nr1d1* (Figure 3, B–D). In stark contrast, *Per1* and *Per2* were both slow to reset in the pancreas, whereas *Nr1d1* adjusted fast (Figure 3E). Of note, PS_{50} values in Figure 3E were reconfirmed by repeated analysis yielding a *P* value of 0.05 or less for *Nr1d1* versus *Per2*.

Our quantitative analysis of the rate by which clock gene expression rhythms adapt to an advanced light schedule showed considerable variation between genes and organs. This misalignment in expression rhythms is thus a molecular hallmark of jet lag and a likely cause of its discomfort.

The adrenal clock regulates endocrine and behavioral reentrainment during jet lag. Thus far, we showed that jet lag is characterized by a widespread, transient desynchronization of the molecular clockwork. However, it remains unclear by what mechanism the circadian system becomes realigned. Both the present study and recent work by others (22, 32) showed that the SCN clock adapted fast to the new light schedule. Moreover, we found that such rapid reentrainment was also the case for the adrenal clock. It should be noted that adrenalectomized rats show an accelerated rate of reentrainment (35). Together, these findings raise the possibility that the adrenal clock contributes in a critical way to resynchronization. To examine this possibility, we analyzed the role of the adrenal circadian oscillator in our jet lag paradigm. First, we transplanted adrenals from clock-deficient *Per2/Cry1* double-mutant animals into adrenalectomized WT hosts (34), creating adrenal clock–deficient mice (host^{WT}/adrenal$^{Per2/Cry1}$; referred to herein as

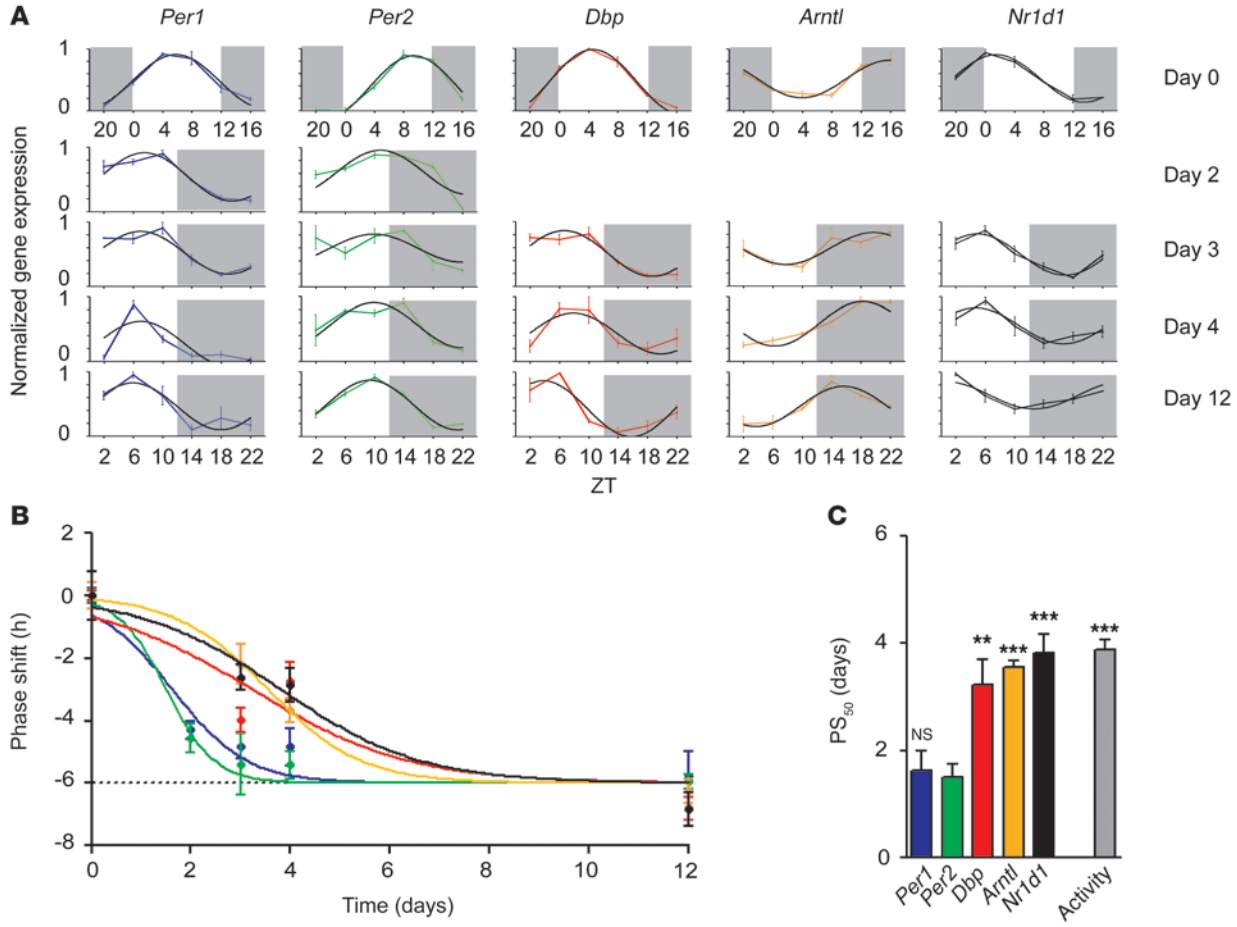

Figure 2

Resetting of clock genes during jet lag in the SCN. (**A**) Diurnal mRNA profiles (average ± SEM) of 5 different clock genes at days 0, 2, 3, 4, and 12 after the LD shift, superimposed with sine wave fits (black). Dark phases are marked by gray shading. 3 animals were used per time point. (**B**) Shifts of gene expression peak times obtained from the ISH data in **A** showed that adaptation to the new light schedule varied for the 5 clock genes (average ± SEM). Colors are as indicated in **A** and **C**. (**C**) PS_{50} values (average ± SEM) of clock genes in the SCN (from **B**) and of activity reentrainment (from Figure 1B). $^{**}P \leq 0.01$, $^{***}P < 0.001$ versus *Per2*. See Supplemental Table 2 for the results of statistical analysis.

$h^{WT}/a^{P2/C1}$). Animals were subjected to a 6-hour phase advance and the reentrainment of locomotor activity was compared with that of sham-operated controls (i.e., h^{WT}/a^{WT}). In the control group, wheel-running activity took approximately 9 days to fully adapt to the new LD cycle, whereas $h^{WT}/a^{P2/C1}$ mice adapted substantially faster, reaching full reentrainment around day 7 (Figure 4, A and B). PS_{50} values of activity onsets were 28.4% less in animals lacking an adrenal clock (h^{WT}/a^{WT}, 4.95 ± 0.07 days; $h^{WT}/a^{P2/C1}$, 3.55 ± 0.08 days; $P < 0.0001$; $F = 161.4$ [1, 266]).

The diurnal secretion rhythm of GCs from the adrenal is regulated by both SCN and adrenal circadian clocks (34, 40, 41). We therefore analyzed whether reentrainment kinetics of adrenal corticosterone rhythms parallel those of activity reentrainment in $h^{WT}/a^{P2/C1}$ animals. Fecal corticosterone excretion rhythms were measured at 4-hour intervals starting on day 0 and ending on day 5 relative to the phase shift. Additional samples were collected at days –5 and 12. Reentrainment kinetics was assessed by determining the shift of the sine-fitted peak time of corticosterone excretion (Supplemental Figure 2). We found that the reentrainment of hormonal rhythms was significantly accelerated in mice lacking an adrenal clock (Figure 4C). On average, the PS_{50} values were reduced 36% in $h^{WT}/a^{P2/C1}$ animals (h^{WT}/a^{WT}, 2.47 ± 0.17 days; $h^{WT}/a^{P2/C1}$, 1.57 ± 0.10 days; $P < 0.0001$; $F = 22.05$ [1, 84]).

In both experimental groups, shifting of the GC rhythm preceded shifting of activity (Figure 4, compare B and C). This became particularly obvious by plotting locomotor activity onsets against hormonal peak time for transient days 1–5 for each of the 23 animals (Figure 4D). This graph revealed a strong correlation between both parameters (h^{WT}/a^{WT}, $r^2 = 0.79$; $h^{WT}/a^{P2/C1}$, $r^2 = 0.87$). Almost all data points were located above the normal diagonal, reiterating that corticosterone concentration rhythms shift preceded that of locomotor behavior at all times. Figure 4D also shows data points for untreated (UT; i.e., nonoperated) mice; even in this case, shifting of hormone rhythms preceded activity shifts ($r^2 = 0.65$).

In summary, the lack of an adrenal circadian clock accelerated phase-shifting of an important endocrine factor (corticosterone) and of locomotor activity. Because the GC phase shift preceded that of activity, this suggests that hormonal cues act as regulators of behavioral adaptation.

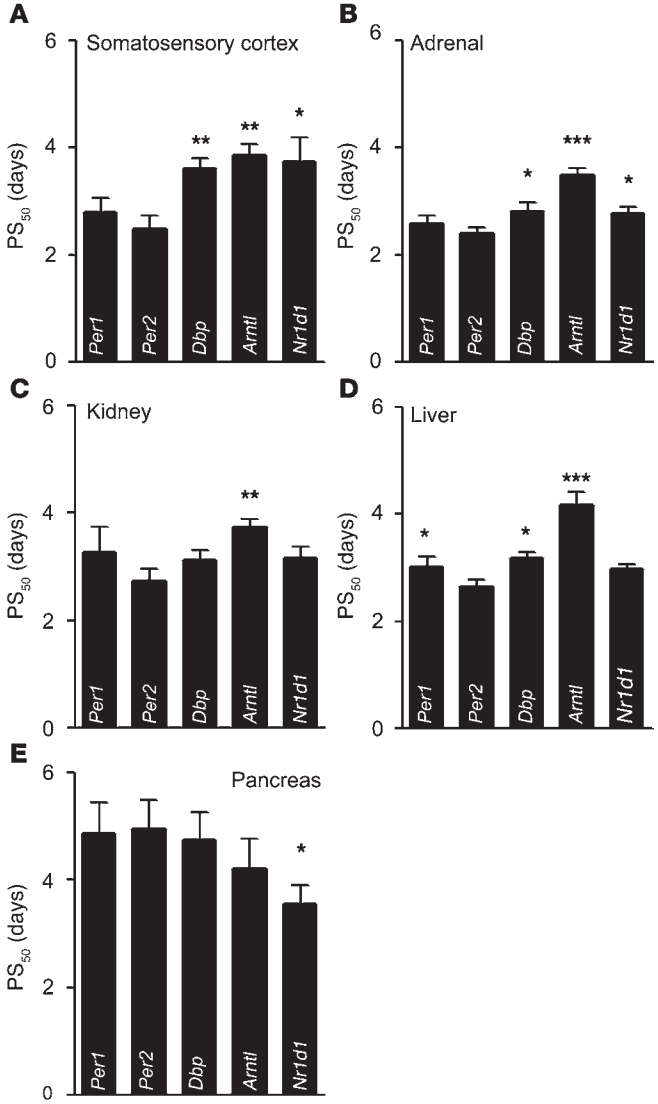

Figure 3
Clock gene resetting kinetics in different tissues following 6-hour LD phase advance. Resetting is represented by PS_{50} values (average ± SEM). $^{*}P \leq 0.05$, $^{**}P < 0.01$, $^{***}P < 0.001$ versus *Per2*. Determination of PS_{50} values from expression data (Supplemental Figure 1; $n = 3$ animals per time point) was done as described in Figure 2. See Supplemental Table 2 for statistical analysis. (**A**) In the somatosensory cortex, similar and rapid adaptation of the *Per1* and *Per2* was followed by slower adaptation of *Dbp*, *Arntl*, and *Nr1d1*. (**B**) In the adrenal, *Per1* and *Per2* both showed comparable and fast adaptation, whereas *Dbp* and *Nr1d1* rhythms shifted at a similar, but slower, rate. *Arntl* showed the slowest adaptation, with a PS_{50} value of 3.5 ± 0.2 days. (**C**) A similar hierarchy was observed for kidney, with fast adaptation for *Per*, *Dbp*, and *Nr1d1*, and a slow one for *Arntl*. (**D**) In liver, *Per2* expression shifted significantly faster than that of the other clock genes except *Nr1d1*. *Per1* and *Dbp* followed at comparable speed, while *Arntl* adapted slowest (4.1 ± 0.2 days). (**E**) In the pancreas, *Per1* and *Per2* shifting was slow, with PS_{50} values of 4.8 ± 0.7 and 4.8 ± 0.7 days, respectively, followed by *Dbp* and *Arntl*. *Nr1d1* adaptation was fastest in this tissue, with a PS_{50} value of 3.5 ± 0.4 days.

GC rhythms regulate reentrainment of locomotor activity. The possible role of adrenal GCs in mediating resynchronization offers an opportunity for experimental control of adjustment to jet lag. To manipulate endogenous GC circadian profiles in mice, we injected MET, which inhibits adrenal 11β-hydroxylase, an enzyme that converts 11-deoxycorticosterone to corticosterone. MET was administered for 16 days at 2 different time points. One group of animals received daily i.p. injection of MET during their inactive day phase, the other at the beginning of their active phase during the night (referred to herein as MET_D and MET_N, respectively; see Methods). Although this injection caused transient drowsiness, it had no effect on the onset of wheel-running activity of MET_D mice, and only minor effect on the onset of MET_N mice (Figure 5, C and D). UT and saline-injected animals (referred to herein as SAL_D and SAL_N) were used as controls.

On the day prior to the phase shift (i.e., day 0), the corticosterone maximum in MET_D mice was forward shifted by 1 hour relative to the SAL_D control (from approximately ZT17 to approximately ZT16; Figure 5A). Conversely, MET_N mice showed peak corticosterone concentration at ZT18, corresponding to a 1-hour backward shift relative to SAL_N (Figure 5B). Of note, MET affected GC peak times, but did not significantly change the amplitude of GC excretion rhythms (data not shown). Sample actograms and activity onset plots emphasized that at the behavioral level, MET_D mice showed accelerated activity resetting, whereas MET_N animals reentrained slower (Figure 5, C–F).

To test whether MET also influences resetting in a phase delay (westward traveling), we combined the above-described MET injection studies with an 8-hour phase delay of the LD cycle. MET_D and MET_N animals shifted the rhythm of corticosterone secretion in a direction reminiscent of the phase-advance studies. After the LD shift, control mice entrained to the new LD cycle within 4–5 days (Figure 6, A and B). MET_D mice showed decelerated adaptation, whereas MET_N animals exhibited more rapid behavioral adaptation (Figure 6, C and D), indicating that the direction of the shift of the corticosterone peak time prior to jet lag determines the effect of MET treatment on behavioral reentrainment. Taken together, our data show that preconditioning mice by timed application of a GC synthesis inhibitor influences the rate of behavioral resynchronization processes that follow a phase advance or delay.

Discussion

Jet lag arises from a transient misalignment of the endogenous circadian timing system with external time (2). We have determined organ-specific expression profiles of key circadian clock genes to characterize circadian resynchronization during jet lag at the molecular level. Each of the organs and clock genes examined showed a characteristic time course of adjustment from the pre– to the post–jet lag state. Therefore, jet lag evokes a global desynchronization of clock gene expression rhythms that gradually returns to the robust alignment typical for the entrained state of the circadian oscillator system. We showed that during this process, the circadian clock of the adrenal gland has a special role, in that adrenal clock–controlled GCs regulated the reentrainment of locomotor activity rhythms. By timed application of MET prior to jet lag, the phase of the endogenous GC rhythm was shifted, which in turn evoked a predictable change in the rate of behavioral reentrainment. Our study thus not only substantiated the importance of GC rhythms in jet lag adaptation, but also established an informative experimental animal model to explore the treatment of jet lag and its associated symptoms.

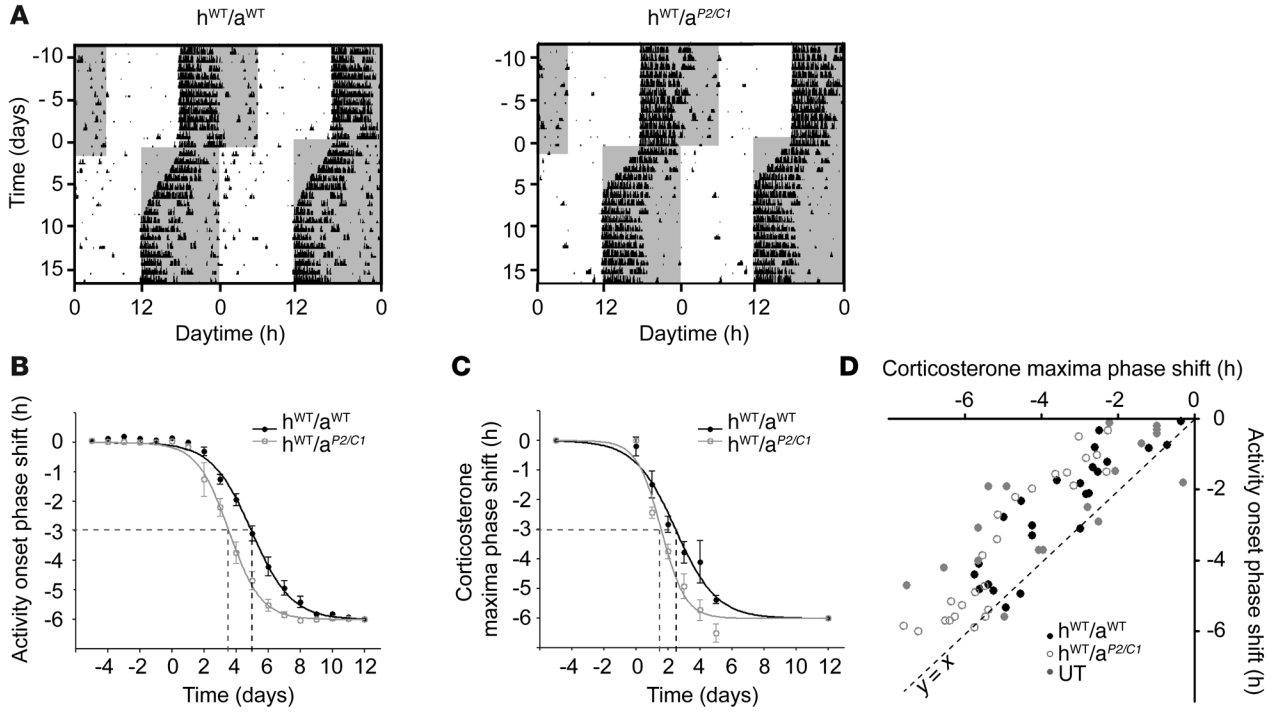

Figure 4

Influence of adrenal clock function on activity reentrainment after 6-hour phase advance of the LD cycle. (**A**) Representative double-plot actograms of h^{WT}/a^{WT} and $h^{WT}/a^{P2/C1}$ animals. Dark phases are denoted by gray shading. (**B**) Resetting kinetics of activity onsets (average ± SEM). The curves differed significantly between days 3 and 8 ($0.003 \le P \le 0.016$). On average, PS_{50} values of activity resetting were reduced by 28.4% for $h^{WT}/a^{P2/C1}$. $n = 9$ (h^{WT}/a^{WT}); 8 ($h^{WT}/a^{P2/C1}$). (**C**) Resetting kinetics of corticosterone excretion maxima peak times (average ± SEM). The curves differed significantly between days 2 and 5 ($0.030 \le P \le 0.004$). On average, PS_{50} values of corticosterone resetting were reduced by 36.5% in $h^{WT}/a^{P2/C1}$. $n = 5$ (h^{WT}/a^{WT}); 6 ($h^{WT}/a^{P2/C1}$). (**D**) Corticosterone maxima and activity onset phase shifts are plotted against each other for individual UT, h^{WT}/a^{WT}, and $h^{WT}/a^{P2/C1}$ mice. Because nearly all individual experimental values were located above the normal ($y = x$; dashed line), corticosterone concentration rhythms shifted more rapidly than did locomotor behavior at all times. A strong correlation between both factors for all groups was found (UT, $r^2 = 0.65$; h^{WT}/a^{WT}, $r^2 = 0.79$; $h^{WT}/a^{P2/C1}$, $r^2 = 0.87$). UT activity is as shown in Figure 1.

Clock gene desynchronization during jet lag differentially affects tissues. To date, surprisingly little is known about the molecular processes underlying resynchronization of internal and external rhythms during jet lag. Pioneering studies with rodents expressing a period gene–driven luciferase reporter have provided inroads to understanding the underlying mechanism (22). It was proposed that overall clock resetting is initiated at the level of the SCN, with rapid reentrainment of period gene rhythms followed by that of cryptochrome genes (32). Reddy and colleagues provide evidence that cryptochrome rhythm entrainment closely correlates with that of behavior (32). Another aspect of perturbation was shown within the SCN itself, where cells can be separated in ventral and dorsal regions that show different resetting kinetics during the period of desynchrony (31).

Here we showed that the order of clock gene resetting varied considerably among different organs, indicative of tissue-specific pathways of reentrainment. Our data distinguish 3 different resetting groups: a CNS group, including the SCN and the somatosensory cortex, with fast responding period genes and slower, but comparably fast, readjustment of *Dbp*, *Arntl*, and *Nr1d1*; a group of peripheral tissues, such as the kidney and the liver, entraining via fast *Per2*, intermediate resetting of *Per1*, *Dbp*, and *Nr1d1*, and slow entrainment of *Arntl*; and the pancreas, showing an inversed order of clock gene resetting, with fast *Nr1d1* and slow *Per1*, *Per2*, *Dbp*, and *Arntl* adaptation. The adrenal clock has an intermediate position between the first (CNS) and the peripheral reentrainment group, in agreement with its previously reported direct light entrainability (34, 41).

Our data thus indicate that the resetting mechanisms underlying the entrainment of peripheral clocks are highly tissue specific. In a similar paradigm in which animals were shifted from a long to a short photoperiod, differential resetting mechanisms were seen between the SCN and the liver (42). This study, as well as the present one, found that *Per2* and *Nr1d1* in the liver, but not in the SCN, shifted at comparably fast speeds. Such differential clock gene resetting lends further support to the hypothesis of differential and tissue-specific reentrainment. Interestingly, we found that the pancreas showed the slowest resetting kinetics of all tissue clocks analyzed in this study. This agrees with the finding that this organ has an exceptionally robust pacemaker (43, 44). Similar to the directly light-activated period genes in the SCN (45), fast shifting of *Nr1d1* rhythms in the pancreas indicated that this gene might be an early target of resetting stimuli in this tissue. Several studies have characterized the nuclear orphan receptor *Nr1d1* as a link between metabolic and circadian regulation (46–49); hence, *Nr1d1* may be a metabolic sensor setting the circadian clock in the pancreas.

The adrenal clock regulates reentrainment during jet lag. We and others have previously shown that the adrenal clock gates the response of the steroidogenic machinery to adrenocorticotropin and thereby

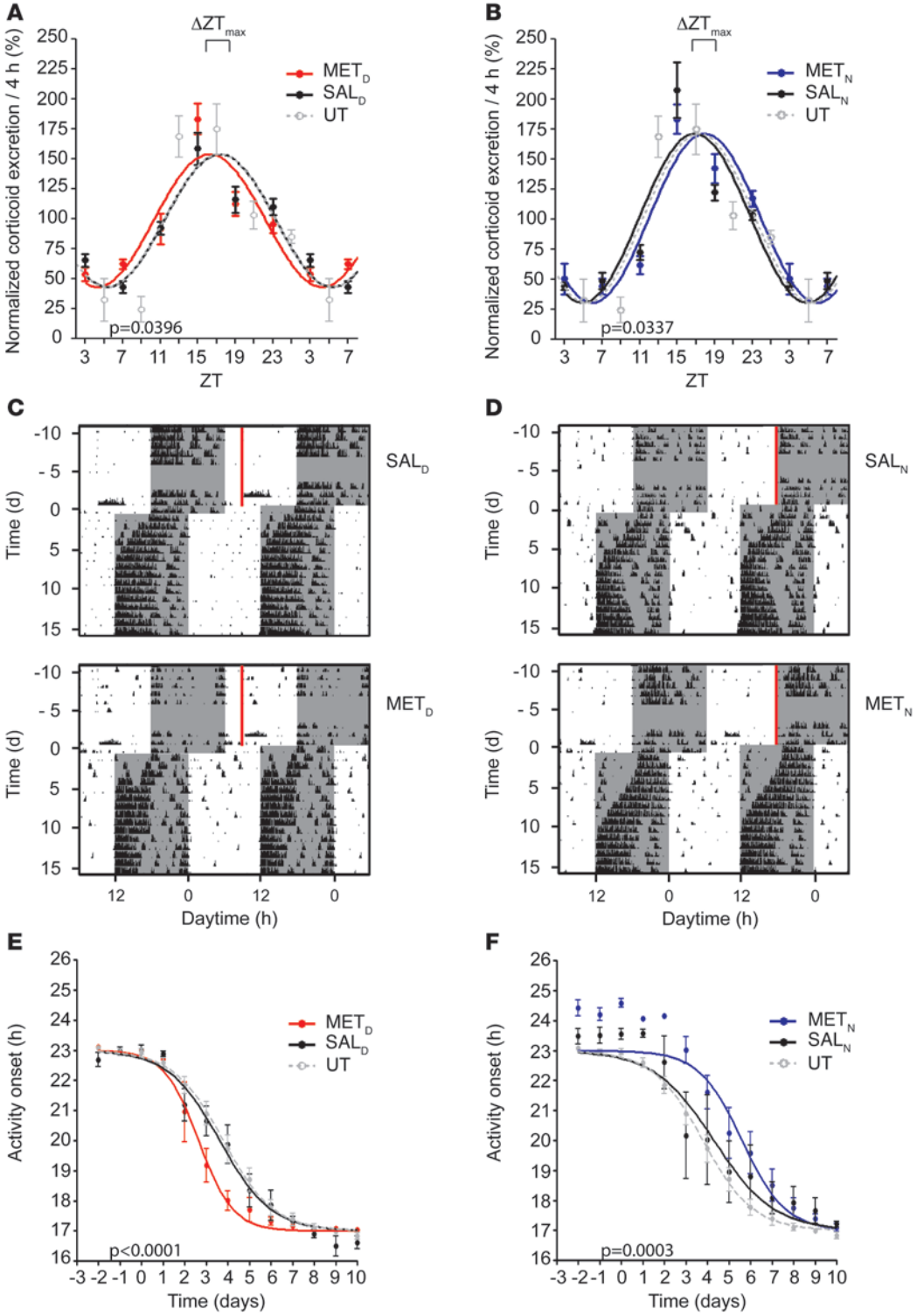

Figure 5

Shifting corticosterone rhythms prior to jet lag affects behavioral resetting kinetics in a phase-advance paradigms. (**A** and **B**) Advanced and delayed corticosterone excretion rhythms of WT MET_D (**A**) and MET_N (**B**) mice after 16 days of MET treatment. The direction of the shift of the corticosterone peak time prior to jet lag in treated mice in comparison to the peak time in SAL_D, SAL_N, and UT control mice (n = 5) is indicated (ΔZT_{max}). (**C** and **D**) Representative double-plotted actograms of SAL_D and MET_D mice (**C**) and SAL_N and MET_N mice (**D**) 2 weeks before and 2 weeks after a 6-hour phase advance of the LD cycle. Time and duration of MET treatment is shown by red bars. Dark phases are denoted by gray shading. (**E** and **F**) Resetting kinetics of activity onsets of MET_D and SAL_D mice (**E**), MET_N and SAL_N mice (**F**), and UT controls. Resetting kinetics of injected animals differed significantly from that of saline-treated animals ($P < 0.0001$, MET_D vs. SAL_D; $P = 0.0003$, MET_N vs. SAL_N; n = 6 per group). All values are average ± SEM.

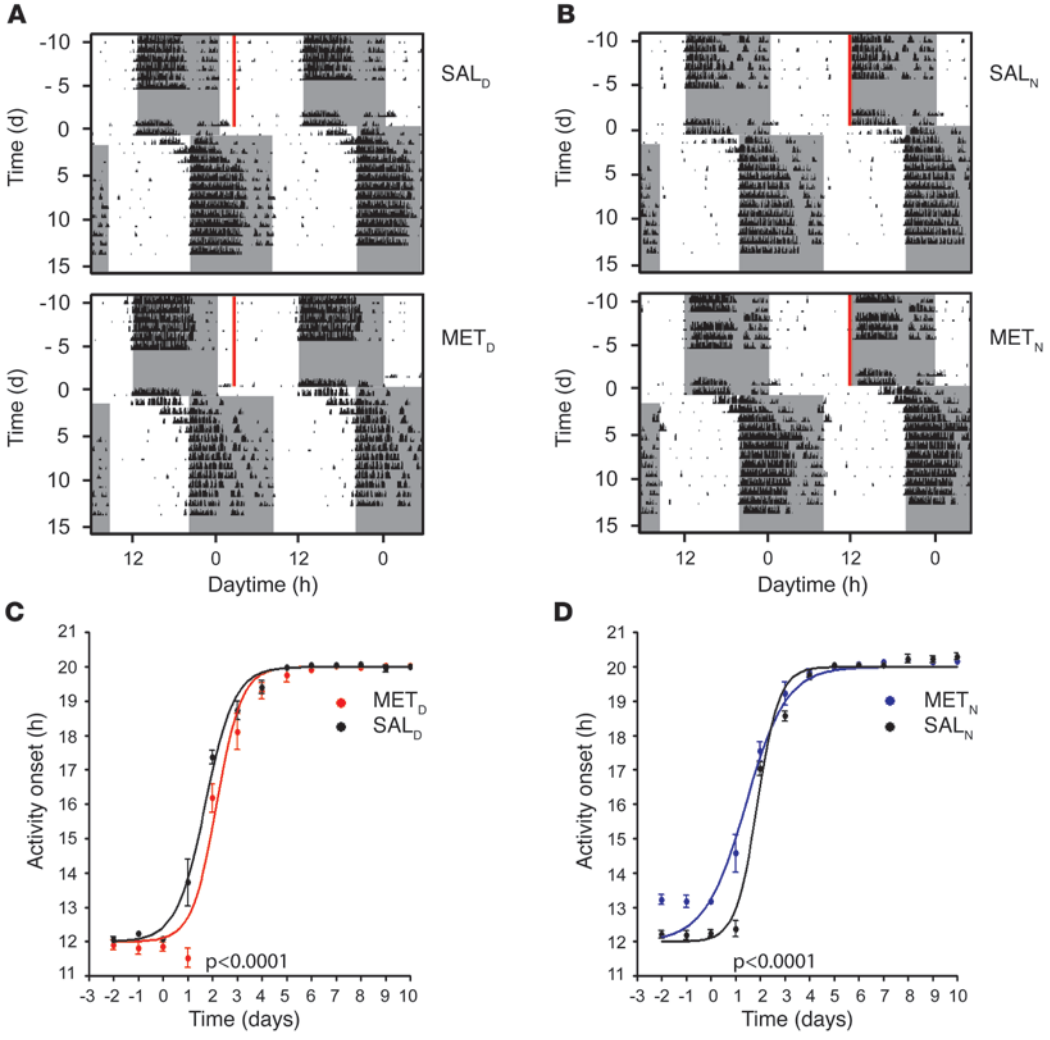

Figure 6

MET injection prior to jet lag affects behavioral resetting kinetics in a phase-delay paradigm. After injection of MET or saline for 16 days, animals were released into an 8-hour phase delay paradigm. (**A** and **B**) Representative double-plotted actograms of SAL_D and MET_D mice (**A**) and SAL_N and MET_N mice (**B**) 2 weeks before and 2 weeks after 8-hour phase delay of the LD cycle. Time and duration of MET treatment is shown by red bars. Dark phases are denoted by gray shading. (**C** and **D**) Resetting kinetics of activity onsets of MET_D and SAL_D mice (**C**) and MET_N and SAL_N mice (**D**). The curves of injected animals differed significantly from that of saline-treated control animals ($P < 0.0001$, MET_D vs. SAL_D and MET_N vs. SAL_N; $n = 6$ per group). Differences between MET- and saline-injected animals were still significant ($P = 0.0105$) when the shift was shortened to 7 hours, caused by delayed onset after MET injection at ZT12. All values are average ± SEM.

influences the rhythm of GC secretion into the blood (34, 40). Moreover, our behavioral data were indicative of a key regulatory function of the adrenal circadian clock in behavioral reentrainment during jet lag. Together with the role of GCs in the resetting of peripheral oscillators (33), these findings suggest a critical role for the adrenal clock in the overall circadian entrainment process (27, 50). Both the SCN and the adrenal clock receive direct photic input through the autonomic nervous system (34, 41), which might account for the rapid entrainment response of these oscillators.

We posit that the SCN signals primarily though neuronal connections to the adrenal, thereby regulating adrenal clock gene expression. In turn, the adrenal clock feeds back to the SCN, where it stabilizes SCN-controlled activity rhythms. GCs are part of this adrenal to SCN feedback, which most likely uses indirect pathway of transmission, as SCN neurons themselves do not express GC receptors (33, 51). Such a feedback control mechanism would prevent uncoordinated resetting of the circadian system, for example in response to sporadic light exposure, and thus serves as a protection from Zeitgeber noise. In the case of jet lag, however, this feedback loop becomes a problem, preventing rapid adaptation of behavioral rhythms to the new time zone. When the adrenal clock is compromised, for example by adrenalectomy (35) or transplantation of a clock-deficient adrenal, then adrenal-SCN feedback is affected. The SCN pacemaker thus becomes less resistant to external perturbation and hence more rapidly relays the external resetting signal to subordinated clocks and tissues, resulting in accelerated reentrainment.

In addition to GCs, the adrenal produces several other hormones, such as mineralocorticoids and catecholamines. Hence, deletion of the adrenal clock might have broader consequences

than merely affecting behavioral resetting. Recently it was shown that in clock-deficient mice, there was an abnormally high synthesis of aldosterone, which impaired the renin-angiotensin pathway of the kidney (52). Thus, the adrenal clock might be involved in a feedback loop not only with the SCN, but also with other organs, such as the kidney, thereby regulating kidney physiology.

The phase of GC rhythms regulates reentrainment during jet lag. Common strategies to alleviate jet lag syndrome aim at adjusting the body clock to the new time zone prior to travel (5). Most treatments are based on preflight plans, including long-term light conditioning, sometimes in combination with timed melatonin administration (6). It has recently been shown that in hamsters, the phosphodiesterase inhibitor sildenafil enhances circadian responses to light and accelerates reentrainment after phase advances of the LD cycle (53).

Few studies have addressed GC function in reentrainment during jet lag, focusing on the regulation of the amplitude (35, 54) and phase (35) of diurnal GC secretion. Sage et al. have shown that in adrenalectomized rats, exogenously provided corticosterone restored the rate of reentrainment only when the imposed corticosterone was rhythmic (35). Moreover, these authors showed that when the corticosterone rhythm was out of phase with the LD cycle, overcompensation was seen, with decelerated reentrainment rates. In our study, MET treatment shifted the phase of GC rhythms by only 1 or 2 hours, yet, reminiscent of the findings of Sage et al., we observed a marked effect on photic reentrainment during jet lag. Thus our present study and that by Sage and coworkers (35) underline the importance of GC rhythms for photic adaptation. As an animal model of jet lag, the strategy of applying the 11β-hydroxylase inhibitor MET to a normal animal seems more practical than adrenalectomy followed by imposing an endogenous GC rhythm. To restore such rhythms requires implantation of slow-release pellets and restricted access to corticosterone-supplemented drinking water (35).

Chronopharmacologic manipulation of GC phase prior to jet lag by timed administration of MET was sufficient to substantially accelerate or slow behavioral reentrainment and thus prolong or shorten the duration of jet lag. In another context, concurrent GC administration and electrical stimulation was shown to promote hippocampal synaptic plasticity, whereas treatment with GC prior to stimulation suppressed this effect (55–57). Both cases provide good examples for the clinical importance of timing in the design of therapeutic strategies.

In summary, our data show that in the SCN and in peripheral oscillators, the process of jet lag was characterized by marked heterogeneity of phase resetting of clock genes that operate in the positive and negative branches of the clock. The consequence is a transient misalignment of the transcriptional feedback loops driving the circadian molecular clock that results in deregulation of tissue-specific oscillators (29, 30). Because circadian clocks control a large number of organotypic output genes, jet lag–associated desynchrony of core clock genes across many organs will initiate a chain reaction culminating in transient perturbation of a wide range of physiological outputs. This perturbation alone would be sufficient to explain large aspects of the pathophysiology of the jet lag syndrome.

Because GC rhythmicity markedly influenced photic resetting during jet lag, modulating these rhythms by timed inhibition of GC synthesis might be an attractive therapeutic alternative because of its minor side effects. Since MET is used in the diagnosis of adrenal insufficiency, its efficacy in alleviating jet lag could be investigated in humans. In addition, the mouse model presented in our study may be used for screening for new chronopharmacologic agents to treat the various symptoms of jet lag affecting a large number of travelers and shift workers each day (58).

Methods

Animals. For all experiments, male WT (C57BL/6J) and homozygous *Per2/Cry1* double mutant mice (*Per2*^{tm1Brd}; ref. 59; and *Cry1*^{tm1Jhjh}; ref. 15) of 2–3 months of age were used as described previously (60). All animal experiments were done with prior permission from the Office of Consumer Protection and Food Safety of the State of Lower Saxony and in accordance with the German Law of Animal Welfare. Mice were housed in small groups of 5 or fewer under LD cycle conditions of 12 hours light, 12 hours dark, with food and water ad libitum.

Behavioral analysis. Handling and activity measurements during experiments were performed as described previously (61). Wheel-running activity was analyzed using ClockLab software (Actimetrics). For the jet lag experiment (6-hour rapid advance or 8-hour rapid delay of the LD cycle), animals were single-housed in running wheel–equipped cages for 2 weeks or longer under LD conditions (lights on, ZT0; light intensities of 350 lux). On day 1 of the jet lag, the lights-off time (ZT12) was shifted from 6 PM to 12 AM (phase advance paradigm) or from 6 PM to 2 AM (phase delay paradigm). Using a short day protocol, we defined day 1 as the first advanced dark period (similar to Davidson et al., who used a short night approach in which the first day is defined by the deemed light period; ref. 31; but different from Yamazaki et al., where the following day — corresponding to day 2 in our study — was referred to as day 1; ref. 22). For the delay experiment (8-hour rapid delay of the LD cycle), animals were housed in running wheel–equipped single cages for 2 weeks or longer under LD conditions (lights on, ZT0; light intensities of 50 lux). On day 1 of the jet lag, the lights-off time (ZT12) was shifted from 12 PM to 8 PM. Day 1 was defined here as the day with the first delayed dark period. Animals were synchronized to the new LD regimen for another 2 weeks during which time of wheel-running activity was recorded. Individual activity onsets before and after the shift were determined by visual inspection and averaged over the whole cohort to asses reentrainment rates.

qPCR. Animals were sacrificed at the indicated time points by cervical dislocation before (day 0) and at 4 different days after the phase advance of the LD cycle. Eyes were removed prior to tissue dissection under a 15-W red safety light at time points during the dark phase (45). Tissue samples were dissected and stored frozen in RNAlater (Ambion). Total RNA samples from adrenal, kidney, liver, and pancreas were prepared using RNeasy Micro and Mini Kits (Qiagen). cDNA was synthesized using Thermoscript RT Kit (Invitrogen). qPCR was performed on an iCycler thermocycler (Bio-Rad) with iQ SYBR Green Supermix (Bio-Rad) according to the manufacturer's protocol. Primer sequences and cycle conditions were as detailed previously (34, 62). *Ef1α* was used as standard, and single-well amplification efficiency estimates and relative quantification of expression levels were performed as described previously (63).

ISH. Animals were sacrificed 1 day before (day 0) and at days 2, 3, 4, and 12 after the LD shift, and brains were dissected. Tissues were fixed, dehydrated, and paraffin embedded; 8-μm sections were prepared (64) and stored at –80°C. Sections were hybridized with ^{35}S-UTP–labeled antisense RNA probes for clock gene transcripts (34). Relative quantification of expression levels was performed by densitometric analysis of autoradiograph films using Scion Image software (Scion Corp.; ref. 60).

Adrenal transplantations. Transplantations of adrenal fragments were performed as described previously (34, 65). Briefly, male WT and *Per2/Cry1* double mutant mice of 6–8 weeks were anesthetized by i.p. injection of 100 mg/kg ketamine and 10 mg/kg xylazine. Adrenals were dissected from

mutant animals following medial laparotomy and transplanted underneath the capsule of the kidney of an adrenalectomized WT host animal. Both adrenals were transplanted into a single host. To control for the transplantation procedure, WT animals received their own (i.e., WT) adrenal transplants following adrenalectomy. After the surgery, animals were allowed to recover for 8 weeks under standard LD conditions to ensure complete reinnervation of the transplanted tissues (66).

Hormone measurements. Fecal samples were collected at 4-hour intervals before and after the jet lag treatment using wheel cages equipped with wire grid floors. To rule out stress-induced effects, animals were transferred to the collection cages 3 days prior to the first sampling interval. Fecal samples were stored at –80°C. Corticoid metabolite extraction and quantification by RIA (MP Biomedicals) were performed as described previously (67).

Pharmacologic treatments. Administration of MET (Sigma-Aldrich) to WT mice was done for 16 days prior to the jet lag procedure (see above). Two sets of 24 animals each received MET dissolved in water (100 mg/kg body weight per day) via i.p. injection at different times during the day. Injections were stopped 1 day before the LD shift (day 0). MET_D animals were injected during the first half of their rest phase at ZT3; MET_N animals received MET injections at the beginning of their activity phase at ZT12. At day 16 of the treatment (day –1 relative to LD shift), fecal samples were collected to analyze the phase shift of corticoid excretion rhythms. Saline-treated (0.9% NaCl) WT littermates injected at ZT3 or ZT12 were used as controls for all experiments.

Statistics. Peak time analyses were performed using Prism software (GraphPad). A sine wave equation, y = BaseLine + Amplitude sin (frequency x + PhaseShift), was fitted to the data. For gene expression and corticosterone data, frequency was fixed to 24 hours. Maxima were calculated using the axis section of the second derivative. To determine PS_{50}, a sigmoid dose-response curve with variable slope was fitted to the sine wave maxima (corticosterone), y = Bottom + (Top – Bottom) $(1 + 10^{(\log PS_{50} - x)\ \mathrm{HillSlope}})$, or onset time points (locomotor activity) for each group. To test whether the best-fit PS_{50} values differed between data sets, data were compared by extra sum-of-squares F test using a P value of less than 0.05 as a threshold. Maxima of gene expression or corticosterone at specific days were compared by Mann-Whitney rank sum test, even if normality tests and equal variance tests were positive, reflecting the small sample sizes of 3–9. A statistically significant difference was assumed with P values less than 0.05. Correlations between phase-shift activity onsets and corticosterone maxima were performed using linear regression. The quality of fit was estimated by r determination. Departure from linearity was tested with runs test. Normality and homoscedasticity tests were passed for all data sets. Diurnal variation of expression data was tested using Fourier analysis with CircWave version 3.3 software (34) and threshold values of 0.05 for α and a period of 24 hours.

Acknowledgments

This work was supported by the Max Planck Society. H. Oster is an Emmy Noether fellow of the Deutsche Forschungsgemeinschaft.

Received for publication September 17, 2009, and accepted in revised form May 5, 2010.

Address correspondence to: Gregor Eichele, Department Genes and Behavior, Max Planck Institute for Biophysical Chemistry, Am Fassberg 11, 37077 Göttingen, Germany. Phone: 49.551.201.2701; Fax: 49.551.201.2705; E-mail: geichel@gwdg.de.

1. Arendt J, Marks V. Physiological changes underlying jet lag. *Br Med J (Clin Res Ed)*. 1982;284(6310):144–146.
2. Comperatore CA, Krueger GP. Circadian rhythm desynchronosis, jet lag, shift lag, and coping strategies. *Occup Med*. 1990;5(2):323–341.
3. Tapp WN, Natelson BH. Circadian rhythms and patterns of performance before and after simulated jet lag. *Am J Physiol*. 1989;257(4 pt 2):R796–R803.
4. Cho K, Ennaceur A, Cole JC, Suh CK. Chronic jet lag produces cognitive deficits. *J Neurosci*. 2000;20(6):RC66.
5. Waterhouse J, Reilly T, Atkinson G, Edwards B. Jet lag: trends and coping strategies. *Lancet*. 2007;369(9567):1117–1129.
6. Arendt J. Managing jet lag: Some of the problems and possible new solutions. *Sleep Med Rev*. 2009;13(4):249–256.
7. Haimov I, Arendt J. The prevention and treatment of jet lag. *Sleep Med Rev*. 1999;3(3):229–240.
8. Srinivasan V, Spence DW, Pandi-Perumal SR, Trakht I, Cardinali DP. Jet lag: therapeutic use of melatonin and possible application of melatonin analogs. *Travel Med Infect Dis*. 2008;6(1–2):17–28.
9. Filipski E, et al. Effects of chronic jet lag on tumor progression in mice. *Cancer Res*. 2004; 64(21):7879–7885.
10. Cho K. Chronic 'jet lag' produces temporal lobe atrophy and spatial cognitive deficits. *Nat Neurosci*. 2001;4(6):567–568.
11. Penev PD, Kolker DE, Zee PC, Turek FW. Chronic circadian desynchronization decreases the survival of animals with cardiomyopathic heart disease. *Am J Physiol*. 1998;275(6 pt 2):H2334–H2337.
12. Davidson AJ, Sellix MT, Daniel J, Yamazaki S, Menaker M, Block GD. Chronic jet-lag increases mortality in aged mice. *Curr Biol*. 2006;16(21):R914–R916.
13. Dunlap JC. Molecular bases for circadian clocks. *Cell*. 1999;96(2):271–290.
14. Reppert SM, Weaver DR. Molecular analysis of mammalian circadian rhythms. *Annu Rev Physiol*. 2001;63:647–676.
15. van der Horst GT, et al. Mammalian Cry1 and Cry2 are essential for maintenance of circadian rhythms. *Nature*. 1999;398(6728):627–630.
16. Preitner N, et al. The orphan nuclear receptor REV-ERBalpha controls circadian transcription within the positive limb of the mammalian circadian oscillator. *Cell*. 2002;110(2):251–260.
17. Ripperger JA, Shearman LP, Reppert SM, Schibler U. CLOCK, an essential pacemaker component, controls expression of the circadian transcription factor DBP. *Genes Dev*. 2000;14(6):679–689.
18. Welsh DK, Yoo SH, Liu AC, Takahashi JS, Kay SA. Bioluminescence imaging of individual fibroblasts reveals persistent, independently phased circadian rhythms of clock gene expression. *Curr Biol*. 2004;14(24):2289–2295.
19. Yan L, Miyake S, Okamura H. Distribution and circadian expression of dbp in SCN and extra-SCN areas in the mouse brain. *J Neurosci Res*. 2000;59(2):291–295.
20. Abe H, et al. Clock gene expressions in the suprachiasmatic nucleus and other areas of the brain during rhythm splitting in CS mice. *Brain Res Mol Brain Res*. 2001;87(1):92–99.
21. Tosini G, Menaker M. Circadian rhythms in cultured mammalian retina. *Science*. 1996; 272(5260):419–421.
22. Yamazaki S, et al. Resetting central and peripheral circadian oscillators in transgenic rats. *Science*. 2000;288(5466):682–685.
23. Yoo SH, et al. PERIOD2:LUCIFERASE real-time reporting of circadian dynamics reveals persistent circadian oscillations in mouse peripheral tissues. *Proc Natl Acad Sci U S A*. 2004;101(15):5339–5346.
24. Damiola F, Le Minh N, Preitner N, Kornmann B, Fleury-Olela F, Schibler U. Restricted feeding uncouples circadian oscillators in peripheral tissues from the central pacemaker in the suprachiasmatic nucleus. *Genes Dev*. 2000;14(23):2950–2961.
25. Liu S, Cai Y, Sothern RB, Guan Y, Chan P. Chronobiological analysis of circadian patterns in transcription of seven key clock genes in six peripheral tissues in mice. *Chronobiol Int*. 2007;24(5):793–820.
26. Oishi K, Fukui H, Ishida N. Rhythmic expression of BMAL1 mRNA is altered in Clock mutant mice: differential regulation in the suprachiasmatic nucleus and peripheral tissues. *Biochem Biophys Res Commun*. 2000;268(1):164–171.
27. Schibler U, Ripperger J, Brown SA. Peripheral circadian oscillators in mammals: time and food. *J Biol Rhythms*. 2003;18(3):250–260.
28. Perreau-Lenz S, Pevet P, Buijs RM, Kalsbeek A. The biological clock: the bodyguard of temporal homeostasis. *Chronobiol Int*. 2004;21(1):1–25.
29. Storch KF, et al. Extensive and divergent circadian gene expression in liver and heart. *Nature*. 2002;417(6884):78–83.
30. Panda S, et al. Coordinated transcription of key pathways in the mouse by the circadian clock. *Cell*. 2002;109(3):307–320.
31. Davidson AJ, Castanon-Cervantes O, Leise TL, Molyneux PC, Harrington ME. Visualizing jet lag in the mouse suprachiasmatic nucleus and peripheral circadian timing system. *Eur J Neurosci*. 2009;29(1):171–180.
32. Reddy AB, Field MD, Maywood ES, Hastings MH. Differential resynchronisation of circadian clock gene expression within the suprachiasmatic nuclei of mice subjected to experimental jet lag. *J Neurosci*. 2002;22(17):7326–7330.
33. Balsalobre A, et al. Resetting of circadian time in peripheral tissues by glucocorticoid signaling. *Science*. 2000;289(5488):2344–2347.
34. Oster H, et al. The circadian rhythm of glucocorticoids is regulated by a gating mechanism residing in the adrenal cortical clock. *Cell Metab*. 2006;4(2):163–173.
35. Sage D, et al. Influence of the corticosterone rhythm on photic entrainment of locomotor activity in rats. *J Biol Rhythms*. 2004;19(2):144–156.
36. Stephan FK, Zucker I. Circadian rhythms in drinking behavior and locomotor activity of rats are

eliminated by hypothalamic lesions. *Proc Natl Acad Sci U S A*. 1972;69(6):1583–1586.
37. Sujino M, Masumoto KH, Yamaguchi S, van der Horst GT, Okamura H, Inouye ST. Suprachiasmatic nucleus grafts restore circadian behavioral rhythms of genetically arrhythmic mice. *Curr Biol*. 2003;13(8):664–668.
38. Ralph MR, Foster RG, Davis FC, Menaker M. Transplanted suprachiasmatic nucleus determines circadian period. *Science*. 1990;247(4945):975–978.
39. Sollars PJ, Kimble DP, Pickard GE. Restoration of circadian behavior by anterior hypothalamic heterografts. *J Neurosci*. 1995;15(3 pt 2):2109–2122.
40. Son GH, et al. Adrenal peripheral clock controls the autonomous circadian rhythm of glucocorticoid by causing rhythmic steroid production. *Proc Natl Acad Sci U S A*. 2008;105(52):20970–20975.
41. Ishida A, et al. Light activates the adrenal gland: timing of gene expression and glucocorticoid release. *Cell Metab*. 2005;2(5):297–307.
42. Sosniyenko S, Parkanova D, Illnerova H, Sladek M, Sumova A. Different mechanisms of adjustment to a change of the photoperiod in the suprachiasmatic and liver circadian clocks. *Am J Physiol Regul Integr Comp Physiol*. 2010;298(4):R959–R971.
43. Muhlbauer E, Wolgast S, Finckh U, Peschke D, Peschke E. Indication of circadian oscillations in the rat pancreas. *FEBS Lett*. 2004;564(1–2):91–96.
44. Peschke E, Peschke D. Evidence for a circadian rhythm of insulin release from perifused rat pancreatic islets. *Diabetologia*. 1998;41(9):1085–1092.
45. Albrecht U, Sun ZS, Eichele G, Lee CC. A differential response of two putative mammalian circadian regulators, mper1 and mper2, to light. *Cell*. 1997;91(7):1055–1064.
46. Raghuram S, et al. Identification of heme as the ligand for the orphan nuclear receptors REV-ERBalpha and REV-ERBbeta. *Nat Struct Mol Biol*. 2007;14(12):1207–1213.
47. Yin L, Wang J, Klein PS, Lazar MA. Nuclear receptor Rev-erbalpha is a critical lithium-sensitive component of the circadian clock. *Science*. 2006;311(5763):1002–1005.
48. Meng QJ, et al. Ligand modulation of REV-ERBalpha function resets the peripheral circadian clock in a phasic manner. *J Cell Sci*. 2008; 121(pt 21):3629–3635.
49. Ramakrishnan SN, Muscat GE. The orphan Rev-erb nuclear receptors: a link between metabolism, circadian rhythm and inflammation? *Nucl Recept Signal*. 2006;4:e009.
50. Le Minh N, Damiola F, Tronche F, Schutz G, Schibler U. Glucocorticoid hormones inhibit food-induced phase-shifting of peripheral circadian oscillators. *EMBO J*. 2001;20(24):7128–7136.
51. Rosenfeld P, Van Eekelen JA, Levine S, De Kloet ER. Ontogeny of the type 2 glucocorticoid receptor in discrete rat brain regions: an immunocytochemical study. *Brain Res*. 1988;470(1):119–127.
52. Doi M, et al. Salt-sensitive hypertension in circadian clock-deficient Cry-null mice involves dysregulated adrenal Hsd3b6. *Nat Med*. 2010; 16(1):67–74.
53. Agostino PV, Plano SA, Golombek DA. Sildenafil accelerates reentrainment of circadian rhythms after advancing light schedules. *Proc Natl Acad Sci U S A*. 2007;104(23):9834–9839.
54. Mohawk JA, Cashen K, Lee TM. Inhibiting cortisol response accelerates recovery from a photic phase shift. *Am J Physiol Regul Integr Comp Physiol*. 2005;288(1):R221–R228.
55. Wiegert O, Joels M, Krugers H. Timing is essential for rapid effects of corticosterone on synaptic potentiation in the mouse hippocampus. *Learn Mem*. 2006;13(2):110–113.
56. Alfarez DN, Wiegert O, Joels M, Krugers HJ. Corticosterone and stress reduce synaptic potentiation in mouse hippocampal slices with mild stimulation. *NeuroScience*. 2002;115(4):1119–1126.
57. Pu Z, Krugers HJ, Joels M. Corticosterone time-dependently modulates beta-adrenergic effects on long-term potentiation in the hippocampal dentate gyrus. *Learn Mem*. 2007;14(5):359–367.
58. Wittmann M, Dinich J, Merrow M, Roenneberg T. Social jetlag: misalignment of biological and social time. *Chronobiol Int*. 2006;23(1–2):497–509.
59. Zheng B, et al. The mPer2 gene encodes a functional component of the mammalian circadian clock. *Nature*. 1999;400(6740):169–173.
60. Oster H, Yasui A, van der Horst GT, Albrecht U. Disruption of mCry2 restores circadian rhythmicity in mPer2 mutant mice. *Genes Dev*. 2002;16(20):2633–2638.
61. Jud C, Schmutz I, Hampp G, Oster H, Albrecht U. A guideline for analyzing circadian wheel-running behavior in rodents under different lighting conditions. *Biol Proced Online*. 2005;7:101–116.
62. Oster H, Damerow S, Hut RA, Eichele G. Transcriptional profiling in the adrenal gland reveals circadian regulation of hormone biosynthesis genes and nucleosome assembly genes. *J Biol Rhythms*. 2006;21(5):350–361.
63. Ramakers C, Ruijter JM, Deprez RH, Moorman AF. Assumption-free analysis of quantitative real-time polymerase chain reaction (PCR) data. *Neurosci Lett*. 2003;339(1):62–66.
64. Jakubcakova V, et al. Light entrainment of the mammalian circadian clock by a PRKCA-dependent posttranslational mechanism. *Neuron*. 2007; 54(5):831–843.
65. Musholt TJ, Klebs SH, Musholt PB, Ellerkamp V, Klempnauer J, Hoffmann MW. Transplantation of adrenal tissue fragments in a murine model: functional capacities of syngeneic and allogeneic grafts. *World J Surg*. 2002;26(8):950–957.
66. Ulrich-Lai YM, Engeland WC. Rat adrenal transplants are reinnervated: an invalid model of denervated adrenal cortical tissue. *J Neuroendocrinol*. 2000;12(9):881–893.
67. Abraham D, Dallmann R, Steinlechner S, Albrecht U, Eichele G, Oster H. Restoration of circadian rhythmicity in circadian clock-deficient mice in constant light. *J Biol Rhythms*. 2006;21(3):169–176.